Table IV. $B(\theta) = a \cos^2 \theta + b$[a]

	a	b
experiment[b]	-19.7	15.6
INDO/S'[c] (K_{taut} = 0.35)[d]	-33.7	13.4

[a] Units are $10^{-4}\beta_e D^2/cm^{-1}$. [b] Taken from linear regression in Figure 3. [c] The INDO/S' values of Figure 5 for vertical and horizontal tautomers are used within the approximation that the mole fraction of horizontal tautomers, f_H, is independent of conformer angle. (Relaxing this approximation introduces an angle dependence in a and b too small to detect in the present study.) [d] See footnote 20.

of-plane rotation angle LUMO's for the free acetyl, 35°, is significantly larger than the values from the crystal structure[11] of diacetylporphyrin.[19]

The magnitude of the change in B value associated with rotation about the carbonyl–porphyrin bond is indicated by the a parameter introduced above. The experimentally derived parameters, a and b, are compared in Table IV with values predicted from the INDO/S' results.[20] The angle dependence predicted from INDO is 50% larger than the observed angle dependence.[21]

(18) This was established for **3** on the basis of MCD spectral similarities with those of **1a** in ref 4b.

(19) The small C–C distances in ref 11 between acetyl methyls and side chains on neighboring porphyrins suggest that large intermolecular steric interactions present in the solid state could account for this difference.

(20) In order to compare the INDO/S' results for horizontal and vertical tautomers with experiment, a value of the tautomer equilibrium constant must be specified. $K = 0.35$ is consistent with our earlier MCD studies (ref 4) and with the NMR study of: Schlabach, M.; Wehrle, B.; Limbach, H.-H.; Bunnenberg, E.; Knierzinger, A.; Shu, A.; Tolf, B.-R.; Djerassi, C. *J. Am. Chem. Soc.* **1986**, *108*, 3856–3858.

(21) The comparison is rather sensitive to the value of the tautomer equilibrium assumed, and this difference quickly diminishes as K is increased toward unity.

Conclusions

The B terms extracted from the Q_0^x band MCD of porphyrin derivatives show a sensitivity to structural variations in the chromophore that is both larger and more systematic than that displayed by the comparable integrated quantities in ordinary absorption spectra, the dipole strengths. This sensitivity is most dramatically displayed in the phenomenom of sign inversion, which can be induced in the Q_0^x band of porphyrins by electron-withdrawing π substituents, e.g., in porphyrin **6**. Since the occurrence of sign inversion is also strongly modulated by the position of the central protons, the two effects, electron withdrawal by π substituents and central proton tautomerism, are found to act conjunctively to determine the observed MCD.

This structural sensitivity allows the application of empirical correlations and theoretical models, both simple (Michl[17] perimeter model) and sophisticated (INDO), to the measured MCD to yield information about π-substituent conformation and central proton tautomerism. Rotation angles with respect to the planar of the porphyrin ring were deduced in the present study for carbonyl substituents from variations in the Q_0^x band MCD. The observed angle dependence of MCD was reproduced reasonably well by INDO calculations using assumptions about the tautomer equilibrium derived from previous MCD[4] and NMR[20] studies.

Acknowledgment. We are indebted to Mrs. Ruth Records for MCD measurements, to Professor Peter S. Clezy for porphyrin samples, and to Dr. Steven J. Milder for comments. Financial support for this work was provided in part by grants from the National Institutes of Health (GM-20276) and the National Science Foundation (CHE 80-25733).

Registry No. 1f, 63940-11-4; **3**, 105230-12-4; **4**, 105230-13-5; **5**, 105230-14-6; **6**, 105230-15-7.

S_1 Torsional Potentials of Substituted Anthracenes

David W. Werst, Ann M. Brearley, W. Ronald Gentry,* and Paul F. Barbara*†

Contribution from the Department of Chemistry, University of Minnesota, Minneapolis, Minnesota 55455. *Received June 12, 1985*

Abstract: The vibrational structures of jet-cooled 2-phenylanthracene, 9-vinylanthracene, and 9-(2-naphthyl)anthracene have been investigated by laser-induced fluorescence in the frequency range 29900–27600 cm^{-1}. For each molecule the excitation spectrum contains a progression that can be assigned to an excited-state mode corresponding primarily to torsional motion about the bond joining the anthracene ring to the substituent. The experimentally observed vibrational spacings for this mode are modeled well by a simple one-dimensional effective potential in the torsional angle ϕ, of the form $V(\phi) = {}^1/_2\sum_n V_n(1 - \cos n\phi)$. The best-fit potential parameters for the molecule are the following: 2-phenylanthracene, V_2 = 864 cm^{-1} and V_4 = -77 cm^{-1}; 9-vinylanthracene, V_2 = 1909 cm^{-1} and V_4 = -106 cm^{-1}; and 9-(2-naphthyl)anthracene, V_2 = -1087 cm^{-1} and V_4 = -1000 cm^{-1}. However, a comparison of observed vibronic intensities and isotope shifts in the vibrational spacings with those predicted for pure torsional motion shows that the simple one-dimensional-model potential is not completely adequate.

Torsional motion about single bonds is important in many aspects of the study of chemical structure and dynamics. Torsional potential functions have been studied extensively because they are the dominant factor in determining conformational structure, and because they reflect the operation of chemical forces such as conjugation and repulsive nonbonding interactions. Torsional vibrations typically have very low frequencies. Consequently, they make large contributions to the molecular density of states and free energy. In chemical kinetics, torsional motion is important because it is often a major component of the reaction coordinates of organic chemical reactions, especially isomerization.[1-5]

† Fellow of the Alfred P. Sloan Foundation, 1984–1985, and Presidential Young Investigator, 1984–1989.

(1) (a) Syage, J. A.; Felker, P. M.; Zewail, A. H. *J. Chem. Phys.* **1984**, *81*, 4685. (b) Syage, J. A.; Felker, P. M.; Zewail, A. H. *J. Chem. Phys.* **1984**, *81*, 4706.

(2) (a) Velsko, S. P.; Fleming, G. R. *J. Chem. Phys.* **1982**, *76*, 3553. (b) Loufty, R. O.; Arnold, B. A. *J. Phys. Chem.* **1982**, *86*, 4205. (c) Courtney, S. H.; Fleming, G. R.; Khundkar, L. R.; Zewail, A. H. *J. Chem. Phys.* **1984**, *80*, 4559. (d) Keery, K. M.; Fleming, G. R. *Chem. Phys. Lett.* **1982**, *93*, 322. (e) Shepanski, J. F.; Keelan, B. W.; Zewail, A. H. *Chem. Phys. Lett.* **1983**, *103*, 9.

0002-7863/87/1509-0032$01.50/0

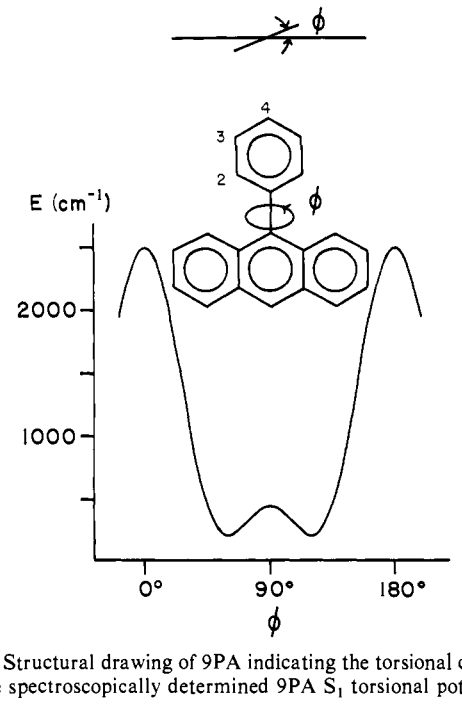

Figure 1. Structural drawing of 9PA indicating the torsional coordinate ϕ and the spectroscopically determined 9PA S_1 torsional potential.[8]

This paper is concerned with torsional motion about bonds between unsaturated groups and aromatic rings, such as the torsional coordinate ϕ of 9-phenylanthracene as shown in Figure 1. Vibrational modes of this type, which involve small torsional barriers and large reduced masses (moments of inertia), have low vibrational frequencies ($\lesssim$80 cm^{-1}) and large nuclear amplitudes. Both factors make modes of this type difficult if not impossible to study by conventional Raman and infrared methods. First of all, measurements must be made on gas-phase samples to avoid the tremendous perturbations that have been observed for large-amplitude, torsional vibrations of molecules in condensed phases.[6,7] However, at temperatures high enough for the vapor pressure to be sufficient for spectroscopic measurements, the low-frequency region of the vibrational spectrum is in general greatly congested due to thermally excited rotational and low-frequency vibrational levels.

Recent papers from our laboratory[8,9] and others[10] have demonstrated an effective alternative to infrared and Raman spectroscopy for the study of the torsional vibrations of aromatic molecules. We have studied vibrations of this type by vibronic spectroscopy of samples which are seeded into supersonic expansions of He in order to simplify the spectra by reducing rotational and vibrational congestion., For example, Werst, Gentry, and Barbara studied the torsional vibration of 9-phenylanthracene (9PA) by laser induced fluorescence (LIF) spectroscopy.[8] Under extreme molecular beam cooling conditions a progression was identified in the LIF spectrum and assigned to a torsional mode of the first excited electronic singlet state S_1. The observed torsional energy levels were fitted well with a one-dimensional potential of the simple form

$$V(\phi) = \tfrac{1}{2}\sum_n V_n(1 - \cos n\phi) \qquad (1)$$

Here ϕ is the angle about the bond joining the aromatic rings. The best-fit effective potential of 9PA is shown in Figure 1. The larger barriers at 0° and 180° are a result of the periplanar repulsion of the H atoms that are closest in the planar geometry of 9PA. The barrier at 90° is due to a loss in resonance stabilization between the aromatic rings in the perpendicular geometry of 9PA. The torsional potential of ground-state S_0 9PA was also determined by the LIF technique as discussed below and elsewhere.[8]

Potentials of the type shown in Figure 1 should be viewed as effective potentials in which there are small adiabatic displacements in other modes of much higher frequency. The underlying assumption is that the torsional mode is approximately separable from all of the higher frequency modes of the molecule.[11] The Hamiltonian that corresponds to this model is

$$H = \frac{-d}{d\phi}[F(\phi)]\frac{d}{d\phi} + \tfrac{1}{2}\sum_n V_n(1 - \cos n\phi) \qquad (2)$$

where $F(\phi) = h/8\pi cI(\phi)$ and I is the reduced moment of inertia for the rigid-rotor torsion as described by Pitzer.[12] The angular dependence of I is small, so it is a good approximation to treat F as a constant.

The previous papers that we published on the determination of torsional potentials by LIF spectroscopy dealt with (i) investigating the validity of the one-dimensional fitting technique[9] and (ii) exploring the electronic state dependence of the torsional potentials of 9PA.[8] The present paper is concerned with the effect on the torsional potentials of varying the substituent and position of substitution. The torsional potentials of three molecules are described in this paper: 9-vinylanthracene (9VA), 9-(2-naphthyl)anthracene (9(2N)A), and 2-phenylanthracene (2PA). Less extensive LIF results on 9-methylanthracene and 2-methylanthracene are also reported. These results are useful for several reasons. First, they allow us to examine the validity of the torsional separability assumption for cases of lower symmetry than 9PA. Second, the theoretical calculation of torsional potentials is a subtle and challenging problem, and these data provide benchmarks for comparison. Third, information on the torsional potentials and energy levels for the isolated gas-phase molecule provides a valuable point of reference for spectroscopic studies of isomerization reactions of similar species in solution.

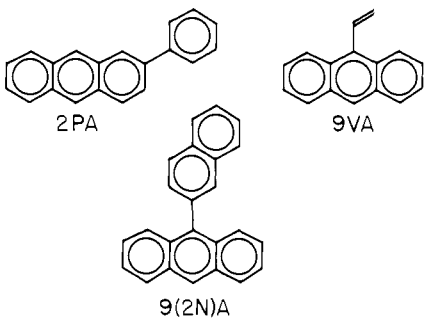

Experimental Section

The experimental details of this study are similar to those described previously.[8,9] Briefly, the free-jet source was a variable temperature 70 μs pulsed valve with a 0.5 mm diameter nozzle. The supersonic free jet of He, seeded with the anthracene derivative, was crossed 15 mm from the nozzle by the output of a nitrogen laser-pumped dye laser. The total induced fluorescence was collected by a single $f/1.5$ lens and detected

(3) (a) El-Bayoumi, M. A.; Halim, F. M. A. *J. Chem. Phys.* **1968**, *48*, 2536. (b) Barbara, P. F.; Rand, S. D.; Rentzepis, P. M. *J. Am. Chem. Soc.* **1981**, *103*, 2156.
(4) Brearley, A. M.; Strandjord, A. J. G.; Flom, S. R.; Barbara, P. F. *Chem. Phys. Lett.* **1985**, *113*, 43.
(5) Flom, S. R.; Brearley, A. M.; Kahlow, M. A.; Nagarajan, V.; Barbara, P. F. *J. Chem. Phys.* **1985**, *83*, 1993.
(6) Baca, A.; Rossetti, R.; Brus, L. E. *J. Chem. Phys.* **1970**, *70*, 5575.
(7) Ball, J. A.; Kahlow, M. A.; Werst, D. W.; Barbara, P. J. *J. Phys. Chem.*, to be submitted.
(8) Werst, D. W.; Gentry, W. R.; Barbara, P. F. *J. Phys. Chem.* **1985**, *89*, 729.
(9) Werst, D. W.; Londo, W. F.; Smith, J. L.; Barbara, P. F. *Chem. Phys. Lett.* **1985**, *118*, 367.
(10) (a) Murakami, J.; Ito, M.; Kaya, K. *J. Chem. Phys.* **1981**, *74*, 6565. (b) Jonkman, H. T.; Wiersma, D. A. *Chem. Phys. Lett.* **1983**, *97*, 261. Jonkman, H. T.; Wiersma, D. A. *J. Chem. Phys.* **1984**, *81*, 1573; (c) Okuyama, K.; Hasegawa, T.; Ito, M.; Mikammi, N. *J. Phys. Chem.* **1984**, *88*, 1711.
(11) Durig, J. R. *Vibrational Spectra and Structure*; Marcel Dekker: New York, 1972; Chapter 4.
(12) Pitzer, K. S. *J. Chem. Phys.* **1946**, *14*, 239.
(13) Biehl, R.; Hinrichs, K.; Kurreck, H.; Lubitz, W.; Mennenga, U.; Roth, K. *J. Am. Chem. Soc.* **1977**, *99*, 4278.

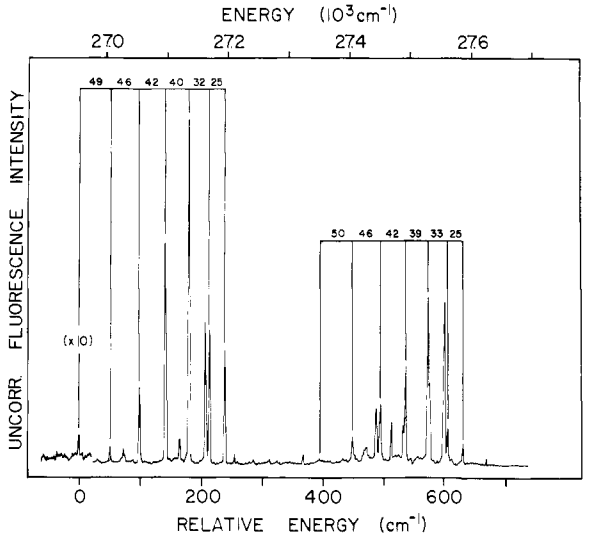

Figure 2. Fluorescence excitation spectrum of 9PA seeded in an expansion of He. The pure torsional progression has been bracketed as well as a second torsional progression appearing in combination with the mode at 387 cm^{-1}.[8] The numbers above the brackets indicate excited state torsional spacings in cm^{-1}.

with a photomultiplier. The bandwidth of the excitation laser was about 1 cm^{-1}.

To obtain the emission spectra of 2PA and 9VA, the fluorescence was dispersed by a grating polychromator (HR320) and detected by a photodiode array–optical multichannel analyzer (PAR Model 1420). The excitation source for the emission experiments was a Nd:YAG laser-pumped dye laser. The detection resolution was 7 cm^{-1}.

The compounds 9-vinylanthracene, 2-methylanthracene, and 9-methylanthracene were purchased from Aldrich and purified by recrystallization from ethanol or chromatography on silica with cyclohexane as the eluent. β-d_2-9VA was synthesized by the method described in ref 14b with use of a deuterated Wittig reagent. 9(2N)A was synthesized by the method described in ref 13, and 2-phenylanthracene was synthesized by the method given in ref 14a. Both compounds were purified by column chromatography with silica and cyclohexane. Purity was verified by comparing the melting points to the values in the literature.

Results and Discussion

A portion of the LIF excitation spectrum of 9PA measured with a He backing pressure of 2.5 atm is given in Figure 2. The specrum of 9PA has been extensively asssigned in a previous paper[8] and is included here for comparison to the spectra of the other substituted anthracenes. The lowest frequency S_1 mode identified in the LIF excitation of 9PA is the torsional vibration in the coordinate ϕ. The pure torsional progression is indicated by the brackets in Figure 2 that begin at the S_1 origin (0 cm^{-1} of excess energy). The numbers above the brackets are the S_1 torsional energy level spacings in wavenumbers. Table I lists the observed torsional energy levels for 9PA and the other substituted anthracenes studied in this paper. The torsional mode for each molecule is labeled T. Torsional progressions in combination with other fundamentals can be found in the spectrum, such as the combination which involves a fundamental at 387 cm^{-1} of excess energy. This set of combination bands is also bracketed in Figure 2. A detailed list of the assignments is given elsewhere.[8] Table II lists the frequencies of the lowest observed transition for the other modes which are denoted by A, B, C, ..., in order of increasing frequency.

Certain features of the spectroscopy of 9PA seem to be typical of biaryl molecules.[8-10] The torsional vibrations of these molecules exhibit relatively long progressions which are found to be active in many regions of the spectrum. Although the torsion is found in combination with other modes, the effective torsional potential does not appear to be a strong function of vibrational excitation in these other modes. Another common feature of the spectroscopy of the biaryl molecules is that the torsional fundamental frequencies are much smaller than most of the other vibrational fundamentals of the molecules. The torsional fundamentals observed to date fall in the range 23–190 cm^{-1}.[8-10]

Figure 3 shows the low-energy portion of the LIF excitation spectrum of 9(2N)A measured with a He backing pressure of 4.5 atm. A study of the transition intensities as a function of He carrier gas pressure has verified that these lines are transitions from the S_0 ground state. Most of the peaks in the spectrum are due to a progression fo a single low-frequency mode alone and in combination with other fundamentals. By analogy to 9PA, we assign this mode to the S_1 torsional vibration. A complication with the interpretation of the LIF spectrum of 9(2N)A and other 9-substituted anthracenes is that the O_0^0 transition of these

Table I. Experimental and Calculated S_1 Torsional Energy Levels

molecule	assignment	$\Delta\nu_{expt}$,[a] cm^{-1}	$\Delta\nu_{calcd}$, cm^{-1}
9PA[b]	T_0^1	49	47.7
	T_0^2	95	93.3
	T_0^3	137	136.4
	T_0^4	177	176.0
	T_0^5	209	208.4
	T_0^6	234	234.6
9(2N)A	T_0^1	33	33.9
	T_0^2	67	67.3
	T_0^3	100	100.3
	T_0^4	133	132.9
	T_0^5	165	165.0
	T_0^6	197	196.7
	T_0^7	228	227.9
2PA	T_0^1		23.3
	T_0^2	47	46.7
	T_0^3		70.2
	T_0^4	94	93.8
	T_0^5		117.5
	T_0^6	141	141.2
	T_0^7		164.9
	T_0^8	188	188.6
	T_0^9		212.3
	T_0^{10}	236	236.0
9VA	T_0^1		66.8
	T_0^2	134	133.5
	T_0^3		200.0
	T_0^4	266	266.2
	T_0^5		332.2
	T_0^6	398	397.9
	T_0^7		463.2
	T_0^8	528	528.2
	T_0^9		592.7
	T_0^{10}	657	656.8

[a] The frequencies are measured from the vibrationless level of the S_1 state, i.e., the zero-point level of the torsional potential. They have been vacuum corrected and have an experimental uncertainty of about ±1 cm^{-1}. For tables of other spectral lines, see Supplementary Material. [b] From ref 8.

Table II. Lowest Observed Transition Frequency (cm^{-1}) for the Observed S_1 Modes of 9PA, 9(2N)A, 2PA, and 9VA

9PA[a]	9(2N)A	2PA	9VA
161 (B)	13 (A)	37 (B)	50 (A)
203 (C)	59 (C)	78 (C)	90 (C)
357 (D)	138 (D)	152 (D)	209 (D)
387 (E)	153 (E)	219 (E)	280 (E)
427 (F)		254 (F)	365 (F)
503 (G)		287 (G)	506 (G)
		413 (H)	613 (H)
		429 (I)	771 (I)
		442 (J)	
		486 (K)	

[a] From ref 8.

(14) (a) Scholl, R.; Neovius, W. *Berichte* **1911**, *44*, 1075. Dickerman, S. C.; de Souza, D.; Wolf, P. *J. Org. Chem.* **1965**, *30*, 1981. Hirshberg, Y.; Haskelberg, L. *Trans. Faraday Soc.* **1943**, *39*, 45. Cook, J. W. *J. Chem. Soc.* **1930**, 1087. Martin, E. L. *J. Am. Chem. Soc.* **1936**, *58*, 1438. (b) Mosnam, A. D.; Nonhebel, D. C.; Russell, J. *Tetrahedron* **1969**, *25*, 3485.

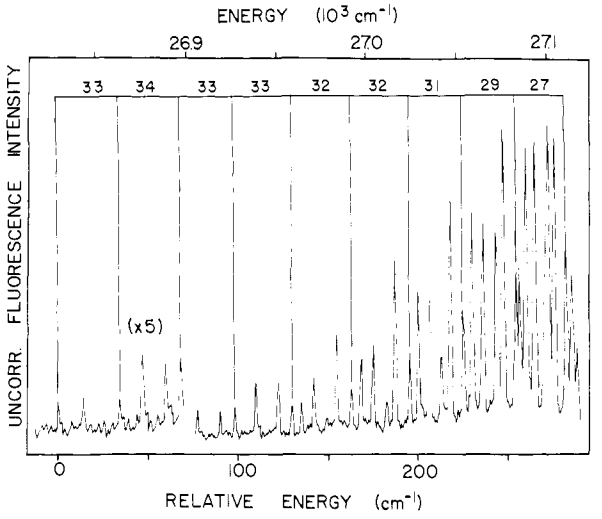

Figure 3. Fluorescence excitation spectrum of 9(2N)A seeded in an expansion of He. One torsional progression is bracketed with excited state torsional spacings shown in cm^{-1}.

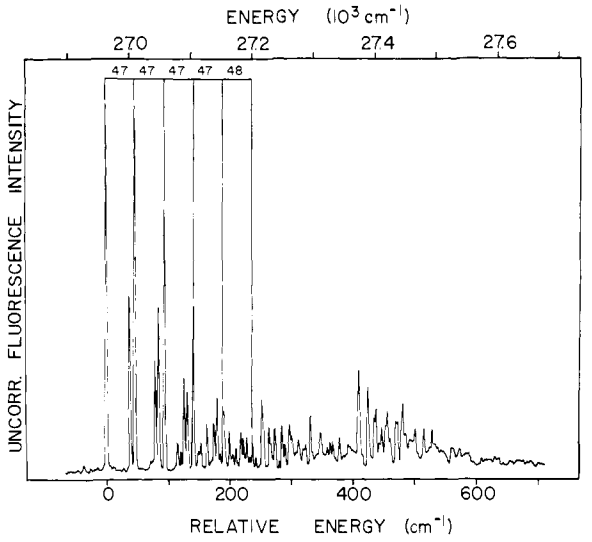

Figure 4. Fluorescence excitation spectrum of 2PA seeded in an expansion of He. One torsional progression is bracketed with excited state torsional spacings shown in cm^{-1}.

molecules is extremely weak due to the Franck–Condon pattern of the excitation spectrum. For example, the O_0^0 transition is so weak for the molecule 9-(3-fluorophenyl)anthracene that the O_0^0 transition is indistinguishable from the background noise in the spectrum.[9] The most important consequence of the uncertainty in whether the true O_0^0 transition has been identified in the spectrum of 9(2N)A is that the list of torsional spacings we have identified in the spectrum may be missing the first and perhaps even the second torsional spacing. The implication of the possibly unobserved lower torsional spacings on the best-fit torsional potentials will be discussed in the Discussion, subsection B.

A total of 41 transitions for 9(2N)A were observed in the frequency range 26800–27200 cm^{-1}. All but one of the vibronic lines could be assigned to the torsional spacings (see Table I), four other fundamentals of S_1 (see Table II), and various combinations of these. The complete list of frequencies and assignments can be found in the supplementary material.

The low excess energy portion of the 2PA LIF excitation spectrum measured with He backing pressure equal to 2.5 atm is shown in Figure 4. Most of the 69 lines that we have identified in the LIF spectrum of the vibrationally cold S_0 molecule are due to a progression in a single low-frequency mode or to progressions in this mode in combination with other fundamentals of S_1 (see Table II). By analogy to other biaryls, we assign the extraordinarily active low-frequency mode to the S_1 torsion. However,

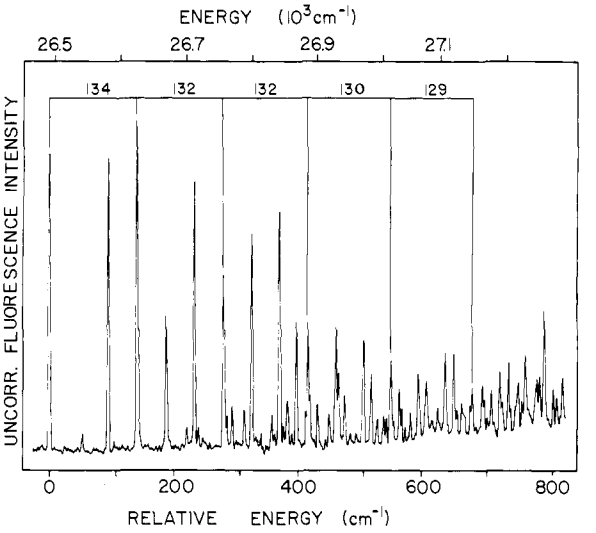

Figure 5. Fluorescence excitation spectrum of 9VA seeded in an expansion of He. One torsional progression is bracketed with excited state torsional spacings shown in cm^{-1}.

an analysis of the symmetry imposed selections rules for the spectroscopy of the biaryl (see Discussion) shows that only even numbered torsional energy levels are allowed in the super-cooled excitation spectrum. Consequently, the torsional energy spacings in the spectrum which are indicated by brackets in Figure 4 correspond to twice the actual spacings between adjacent levels since the odd numbered levels are not observed. This is shown in detail in Table I. The complete list of frequencies and assignments for the observed lines can be found in the supplementary material.

Figure 5 portrays the origin region of the LIF spectrum of 9-vinylanthracene (9VA) measured with a He backing pressure of 3 atm. A study of the LIF spectrum as a function of carrier gas pressure has revealed that the spectrum in Figure 5 is due to vibrationally cold 9VA molecules. Unique among the substituted anthracenes we have studied so far, 9VA possesses two low-frequency modes that show long progressions. Both are nearly harmonic, one with a fundamental frequency of 90 cm^{-1} and one with a fundamental frequency of 134 cm^{-1}.

The existence of two active low-frequency modes in the spectrum might be an indication that 9VA has more than one mode which possesses some component of ϕ motion. We will return to this issue in the Discussion section. Although 9VA may not execute pure ϕ torsional motion, it is worthwhile to try to identify the mode in the spectrum which has the greatest amount of ϕ character. With this goal in mind, we measured the LIF excitation spectrum of β-d_2-9VA. The isotopic shifts for the 90-cm^{-1} mode and the 134-cm^{-1} mode are approximately 2% and 5%, respectively. In the harmonic approximation the fundamental torsional frequencies are proportional to $F^{1/2}$, $\tilde{\nu} = n(V_nF)^{1/2}$.[11] The values of F for 9VA and β-d_2-9VA are listed in Table V. The predicted isotope effects are approximately 11%, which is considerably greater than that observed for either of the 9VA modes.

The small isotope effects on both the 90-cm^{-1} and the 134-cm^{-1} modes suggests that neither is pure torsion. The two 9VA vibrational motions which are probably most strongly coupled to the torsion are the in-plane and out-of-plane bends of the vinyl group. Both are predicted to show smaller β-d_2 isotope effects than the torsion, based on calculations of the rotational moments of inertia of the vinyl group about axes through the ipso carbon and perpendicular to the torsional axis. In the ground state of styrene the in-plane (ν_{29}) and out-of-plane (ν_{41}) bending modes are nearest in frequency to the torsion, which is the lowest frequency mode. Both ν_{29} and ν_{41} of styrene show smaller β-d_2 isotope effects than the torsion.[15] We have assigned the 134-cm^{-1} mode

(15) Gilson, T. R.; Hollas, J. M.; Khalilipour, E.; Warrington, J. V. *J. Mol. Spectrosc.* **1978**, *73*, 234.

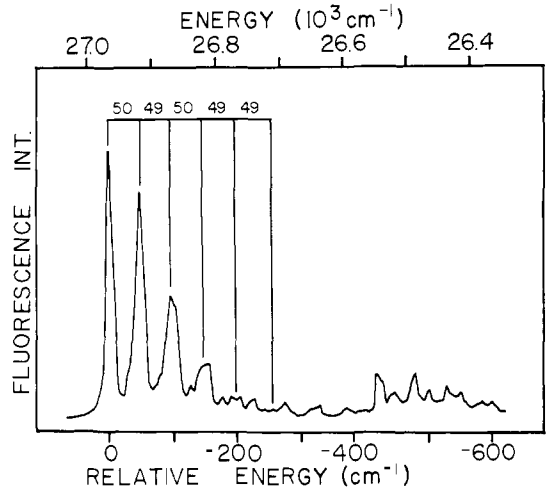

Figure 6. 0^0 level fluorescence of 2PA seeded in an expansion of He. One torsional progression is bracketed with ground state torsional spacings shown in cm^{-1}.

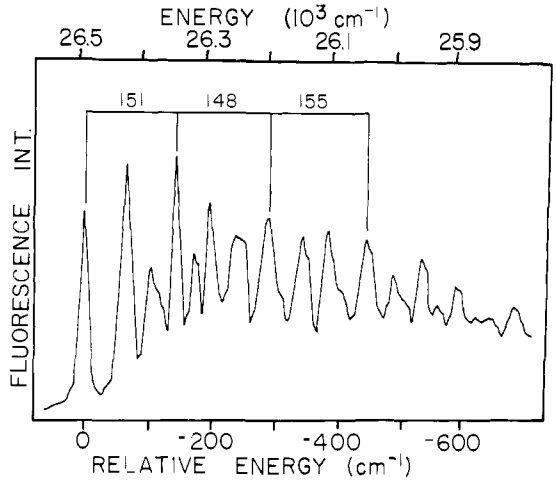

Figure 7. 0^0 level fluorescence of 9VA seeded in an expansion of He. A nearly harmonic progression with ~150-cm^{-1} spacings is bracketed.

of 9VA as the vibration with the largest component of ϕ motion since it shows the largest deuterium isotope effect. This mode will be referred to as the torsional mode in the Discussion section and has been labeled T in Table I. The 90-cm^{-1} mode, which is listed as mode C in Table II, probably involves torsional motion mixed with other large amplitude vibrations such as bending of the single bond that connects the vinyl group to the anthracene ring. One might expect a large coupling between bending and torsional motion since torsional motion undoubtedly modulates the degree of nonbonding interactions between nearby atoms in 9VA, and, in turn, these same nonbonding interactions should be critical factors in determining the bending force constant.

The dispersed emission spectrum of 2PA is displayed in Figure 6. The simple structure of the 2PA emission spectrum is nearly a mirror image of that observed in excitation. By analogy to the assignment of the excitation spectrum, the harmonic 50-cm^{-1} progression has been assigned to even numbered levels of the ground state torsional vibration. Assignments for most of the lines in the 2PA emission spectrum are given in Table III.

The structure in the 9VA emission spectrum (Figure 7) is much more complicated. Assignment is hampered by the congestion of the spectrum and the relatively low resolution (7 cm^{-1}). Although an unambiguous assignment is impossible, we propose the assignment shown in Table IV which uses the same number of vibrational spacings as in the assignment of the excitation spectrum. Some hints can be found of harmonic mode spacings. The four-member progression in the 151-cm^{-1} mode is the longest that has been identified, and it is harmonic within the uncertainty due to the 7-cm^{-1} resolution.

Table III. Dispersed Fluorescence Spectrum and Assignments for 2PA in the Frequency Range 26900–26300 cm^{-1}

ν, cm^{-1}	$\nu(O_0^0) - \nu$, cm^{-1}	assignment
26 969	0	O_0^0
26 918	51	T_2^0
26 869	100	T_4^0
26 841	128	B_1^0
26 819	150	T_6^0
26 791	178	$B_1^0T_2^0$
26 777	192	
26 770	199	T_8^0
26 763	206	
26 742	227	$B_1^0T_4^0$
26 721	248	T_{10}^0
26 693	276	$B_1^0T_6^0$
26 658	311	
26 644	325	$B_1^0T_8^0$
26 602	367	
26 582	387	
26 554	415	C_1^0
26 527	442	D_1^0
26 499	470	$C_1^0T_2^0$
26 478	491	$D_1^0T_2^0$
26 451	518	$C_1^0T_4^0$
26 430	539	$D_1^0T_4^0$
26 396	573	$C_1^0T_6^0$
26 382	587	$D_1^0T_6^0$

[a] Energies are vacuum corrected and have an uncertainty of ±1 cm^{-1}. Spectral resolution was about 1 cm^{-1}.

Table IV. Dispersed Fluorescence Spectrum and Assignments for 9VA in the Frequency Range 26600–25900 cm^{-1}

ν,[a] cm^{-1}	$\nu(O_0^0) - \nu$, cm^{-1}	assignment
26 493	0	O_0^0
26 424	69	A_1^0
26 383	110	B_1^0
26 342	151	C_1^0
26 315	178	$A_1^0B_1^0$
26 288	205	D_1^0
26 247	246	$A_2^0B_1^0$
26 240	253	
26 234	259	$B_1^0C_1^0$
26 194	299	C_2^0
26 139	354	$C_1^0D_1^0$
26 100	393	E_1^0
26 079	414	
26 039	454	C_3^0
26 033	460	$A_1^0E_1^0$
26 000	493	$B_1^0E_1^0$
25 980	513	
25 953	540	$C_1^0E_1^0$
25 927	566	
25 901	592	$D_1^0E_1^0$

Discussion

A. Torsional Levels and Selection Rules. The determination of the effective torsional potentials from a set of experimentally observed torsional energy levels involves three levels of analysis. First, the number of minima in the S_0 and S_1 potentials must be determined, which allows one to choose the appropriate symmetry selection rules for the spectrum that is being analyzed. Second, the torsional spacings are assigned and a best-fit effective torsional potential is determined by variation of parameters. The best-fit potentials at this stage have and arbitrary phase factor in ϕ of 90°. The third step is to determine the phase factor.

The symmetry selection rules for vibronic transitions of the torsion are, of course, based on the usual principle that the product of symmetry species must be totally symmetric, since the $S_0 \rightarrow S_1$ transition is electronically allowed.[16] The appropriate sets of symmetry elements for the problem is two planes of symmetry, at $\phi = 0°$ and $\phi = 90°$. These planes apply to the symmetry of the torsional potential rather than to the equilibrium geometry

(16) Herzberg, G. *Electronic Spectra and Electronic Structure of Polyatomic Molecules*; Van Nostrand-Reinhold: New York, 1966; Chapter 2.

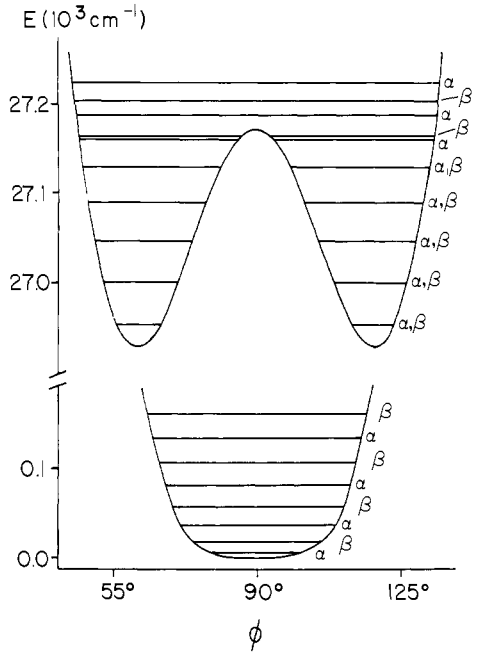

Figure 8. Best-fit S_0 and S_1 torsional potentials of 9PA.[8] Symmetry designations for each level are indicated. α = ss *and* as, β = sa *and* aa.

of the molecule, which may not actually possess these symmetry elements.

A suitable model potential with the required symmetry is given by the function

$$V(\phi) = \tfrac{1}{2}[V_2(1 - \cos 2\phi) + V_4(1 - \cos 4\phi)] \qquad (3)$$

which is a simple case of the more general expression of eq 1. It will be shown below that the V_2 and V_4 terms are sufficient to fit the observed torsional energy level spacings.

Solutions to the Schroedinger equation for the Hamiltonian of eq 2 and the potential of eq 3 are torsional wave functions which are symmetric (s) or antisymmetric (a) with respect to the planes of symmetry at 0° and 90°. A particular torsional level can be assigned a symmetry designation, e.g., ss, where the first and second letters refer to the 0° and 90° symmetry planes, respectively. The allowed transitions in this language are ss ↔ ss, aa ↔ aa, as ↔ as, and sa ↔ sa.

The key to finding the symmetry selection rule for a particular molecule is the identification of the degeneracy of the observed torsional levels. In turn, the determining factor in the degeneracy of the low-lying torsional states is the number of minima in a 360° period of the torsional potential. Here we assume that the torsional degeneracy is not effectively lifted by tunneling, at least for the low-lying torsional levels.

The connection between the number of minima and the torsional degeneracy is nicely demonstrated in the spectroscopy of 9PA. The ground state S_0 potential has *two equivalent* barriers at 0° and 180° and minima at 90° and 270°. The presence of two minima implies that the low-lying levels of S_0 will occur in degenerate pairs with alternating symmetries, as shown in Figure 8. In contrast, the S_1 state has four minima in one period of the potential. The low-lying apparent torsional states in this case have fourfold degeneracy, which span all of the possible symmetry designations.

The apparent selection rule for low-lying torsional states in the LIF excitation spectrum of 9PA is that Δv, the change in apparent torsional quantum number, can be either odd or even. This follows simply from the fact that the vibronic transitions from the lowest apparent level of S_0 (which is doubly degenerate) to any of the fourfold degenerate apparent levels of S_1 are allowed. Of course, the Δv = (even or odd) selection rule breaks down near the top of the 90° barrier and above where mixing begins to lift the degeneracy between states of opposite symmetry with respect to the 90° plane of symmetry. Some care must be taken, but generally it follows that the Δv = (even or odd) rule will hold in any case where at least one of the electronic states has four minima in a period of the potential.

A slightly more complicated situation exists if both S_0 and S_1 torsional potentials have two minima in a period. Symmetry requires that the S_0 and S_1 potentials be related by a constant phase shift, with allowed values 0° or 90°. It can be shown by symmetry that if the phase shift is 0°, then the appropriate selection rule is Δv = even. On the other hand, if the phase shift is 90°, both even and odd values of Δv are allowed.

The determination of whether the torsional potential has two or four minima per 360° period can be made from the anharmonicity of the observed torsional frequencies, independent of selection rule, since the anharmonicities of the two- and four-minima potentials are quite different. In our experience, a given set of torsional frequencies will be fitted well by only one of these assumptions. For an example of the very different anharmonicities obtained with these two types of potentials, consider the level spacings in S_0 and S_1 of 9PA.[8] The negative anharmonicity of the ground state torsional levels requires a flat-bottomed, single-well potential, whereas only a double-well potential (four minima per period) successfully mimics the large positive anharmonicity of the observed excited state spacings.

The observed S_1 torsional frequencies of 9(2N)A, 2PA, and 9VA dictate potentials with four, two, and two minima per period, respectively. As in the case of 9PA, the correct symmetry selection rule for 9(2N)A is Δv = (even or odd) regardless of the shape of the S_0 torsional potential since low-lying levels of the 9(2N)A S_1 potential are fourfold degenerate. A further similarity between 9(2N)A and 9PA is the bell-shaped intensity pattern in the torsional progression. For 9PA this was shown to be the result of an approximately 25° displacement in the equilibrium value of ϕ upon excitation.[8] We can qualitatively infer from the observed 9(2N)A torsional progression intensity pattern that an equally large or slightly larger ϕ displacement exists between the minima of its S_0 and S_1 potentials. The choice of symmetry selection rules for 2PA and 9VA requires knowledge of the shapes of the S_0 torsional potentials (i.e., the degeneracies of the S_0 ground vibrational levels) since the S_1 torsional levels are only doubly degenerate. Ground state torsional frequencies of 2PA measured from the dispersed emission spectrum (Figure 6 and Table I) are harmonic and dictate an S_0 torsional potential with two minima per period. In order to determine the correct selection rule, the relative phase factor between S_0 and S_1 must be established. This is done by seeking agreement between calculated FC factors and observed torsional intensities for a given choice of the relative phase factor, either 0° or 90°. Unfortunately, agreement is not obtained in either case.

This failure to obtain agreement between calculated FC factors and observed torsional intensities must be due to a breakdown of either the one-dimensional torsional model, the FC principle or both. This point will be discussed below. For the present, we make a best guess of the relative phase factor for the purpose of establishing the selection rule. Calculated FC factors (for any choice of Δv) for a relative phase factor of 90° do not put nearly enough intensity in the O_0^0 band and predict a torsional progression with hundreds of lines, while calculated FC factors for a relative phase factor of 0° predict a strong O_0^0 band but not enough intensity in higher members of the progression. A relative phase factor of 0° is more consistent with experiment since it predicts a strong origin band. The discrepancy of the predicted length of the progression might be caused by a small displacement in a different coordinate (e.g., in-plane bend), which is coupled to the torsional motion. The choice of selection rule for 2PA is Δv = even.

On the basis of the presence of harmonic structure in the emission spectrum of 9VA, we infer that its S_0 torsional potential likewise has two minima per 360° period. A relative phase factor between S_0 and S_1 9VA of 0° is deduced by the same reasoning, since the torsional progression intensity patterns in excitation are similar for the two molecules. The choice of selection rule for 9VA is Δv = even.

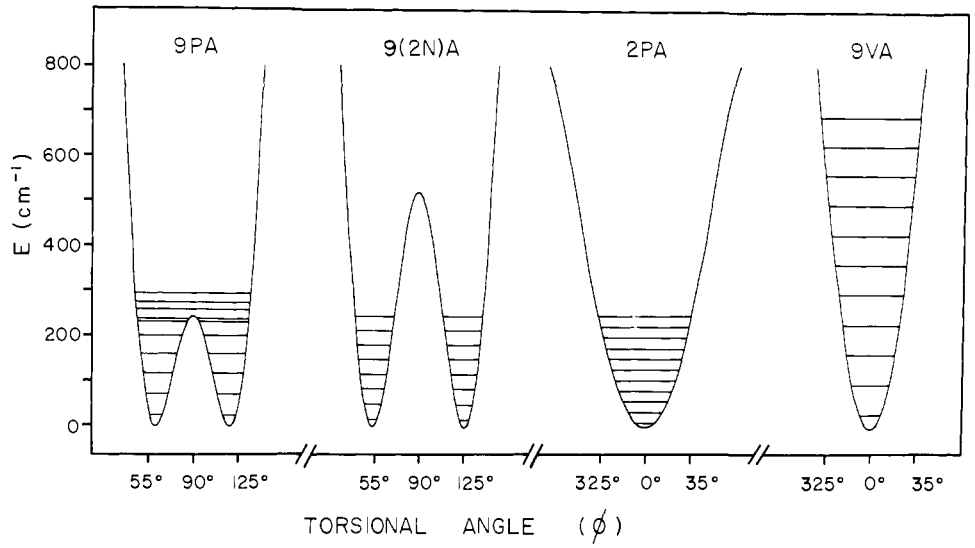

Figure 9. Best-fit S_1 torsional potentials of 9PA,[8] 9(2N)A, 2PA, and 9VA.

Table V. Best-Fit S_1 Torsional Potential Parameters and F Values

molecule	F, cm^{-1}	V_2, cm^{-1}	V_4, cm^{-1}
9PA[a]	0.205	−2055	−1009
9(2N)A	0.0792	−1087	−1000
2PA	0.241	864	−77
9VA	0.755	1909	−106
β-d_2-9VA	0.606		

[a] From ref 8.

B. The Best-Fit Torsional Potentials. Employing the Δv = (even or odd) selection rule for 9(2N)A and Δv = even for 2PA and 9VA we have assigned the observed low-frequency vibrational progressions for the substituted anthracene to apparent torsional energy levels of these molecules. Table I compares the observed frequencies to those from the best-fit effective torsional potential for each molecule. The calculated and experimental frequencies agree within experimental uncertainty. A set of 70 basis functions was used in the calculations. This number was sufficient to achieve convergence of the energy levels in each case. The best-fit potential parameters and F values that were used in the calculations are given in Table V.

The possibly unobserved lower torsional spacings of 9(2N)A mentioned previously would have no effect on the qualitative shape of the 9(2N)A S_1 torsional potential shown in Figure 9. The addition of one or even two lower torsional spacings would merely scale the potential by deepening the double well or, equivalently, increasing the minor barrier.

As state above, the best-fit effective potentials have an arbitrary phase factor of 90°. Fortunately, it is possible to use additional evidence to establish the phase factor for each of the molecules described in this paper. To discuss this further we should consider plots of the low-energy region of the best-fit potentials (which have already been shifted by the appropriate phase factor) for each of the molecules, 9PA, 9(2N)A, 2PA, and 9VA, shown in Figure 9.

We shall employ three separate criteria to establish the correct phase of the torsional potentials: (1) the degree of π resonance in the S_0 and S_1 states, as reflected by the shift in O_0^0 frequency compared to methyl substituted derivatives; (2) the amount of periplanar repulsion of nearby atoms; and (3) the trend toward more planar excited states. Both experiment and theory show that biaryls tend to be more planar in the excited state than in the ground state. Biaryl molecules with experimentally determined geometries include 9PA and biphenyl. 9PA is orthogonal in S_0 and has an equilibrium ϕ value of 61° in S_1.[8] Biphenyl is twisted in S_0 (ϕ = 42°)[17] and planar in S_1.[10a] Theoretical calculations for biaryl molecules predict the same trend. See, for example,

(17) Almenpingen, A.; Bastiansen, O. *K. Nor. Videnski. Selsk. Skr.* **1958**, *4*, 1.

Table VI. $S_0 \rightarrow S_1$ O_0^0 Frequencies of Various Anthracenes

molecule	$\nu(O_0^0)$,[c] cm^{-1}
9PA[a]	26944
d_5-9PA[a]	26940
9-(4-methylphenyl)anthracene[b]	26916
9-(4-fluorophenyl)anthracene[b]	26947
9-(3-methylphenyl)anthracene[b]	26949
9-(3-fluorophenyl)anthracene[b]	26971
9VA	26493
9(2N)A	26837
2PA	26969
9-methylanthracene	26941
2-methylanthracene	27392

[a] From ref 8. [b] From ref 9. [c] Energies are vacuum corrected and have an uncertainty of ±1 cm^{-1}. Spectral resolution was about 1 cm^{-1}.

work by Gustav on biphenyl,[18] 1,1′-binaphthyl,[19] and several phenylnaphthalenes.[20]

To begin the discussion of criterion 1 let us compare the LIF spectra in Figures 2–5 with the spectra of compounds that are not capable of a π resonance interaction between the anthracene group and the substituent. For example, the LIF excitation spectrum of 9-methylanthracene in the excess energy range of less than 600 cm^{-1} contains only about a dozen obsevable transitions.[21] The LIF spectrum of 9-methylanthracene is more sparse because the torsional vibration is not highly active in the spectrum. This undoubtedly reflects the fact that the torsional potential is not a strong function of the electronic state of the molecule due to the absence of ordinary π resonance between the methyl group and anthracene ring.

Another measure of π resonance in the substituted anthracene is the frequency of the O_0^0 transition. It has been suggested previously that the observed shift in the O_0^0 frequency when a conjugated group is substituted for a methyl group in an aromatic molecule is a rough measure of the degree of π resonance through the connecting bond.[22] In particular, when the aromatic ring and substituent are orthogonal, very small shifts are observed. This is the case for the origin of 1,1-∞binaphthyl[10b] which is red shifted only 40 cm^{-1} with respect to that of 1-methylnaphthalene.[23] On the other hand, if the two groups are approximately coplanar, then

(18) Gustav, K.; Sühnel, J.; Wild, U. P. *Helv. Chim. Acta* **1978**, *61*, 2100.
(19) Gustav, K.; Sühnel, J.; Wild, U. P. *Chem. Phys.* **1978**, *31*, 59.
(20) Gustav, K.; Kemka, U.; Sühnel, J. *Chem. Phys. Lett.* **1980**, *71*, 280.
(21) Amirav, A.; Even, V.; Jortner, J. *Anal. Chem.* **1982**, *54*, 1666. Syage, J. A.; Felker, P. M.; Semmes, D. H.; Adel, F. A.; Zewail, A. H. *J. Chem. Phys.* **1985**, *82*, 2896.
(22) Friedel, R. A.; Orchin, M.; Regel, L. *J. Am. Chem. Soc.* **1948**, *70*, 199. Jaffe, H. H.; Orchin, M. *Theory of Ultraviolet Spectroscopy*; Wiley: New York, 1962; Section 15.3.
(23) Warren, J. A.; Hayes, J. M.; Small, G. J. *J. Chem. Phys.* **1984**, *80*, 1786.

the aromatic molecule has a considerably lower O_0^0 frequency. Blue shifts resulting from greater π resonance in S_0 than in S_1 are not expected in light of the trend toward more planar excited states. 1,2′-Binaphthyl and 2,2′-binaphthyl complete a series which nicely demonstrates this trend. Of the three binaphthyls, 2,2′-binaphthyl is expected, for steric reasons, to have the most stable planar configuration, and it has the lowest O_0^0 frequency. 1,2′-Binaphthyl, as expected, falls between the other two.[24]

The O_0^0 frequencies for various substituted anthracenes are given in Table VI. The O_0^0 transitions of the six 9-phenylanthracenes are all within 55 cm^{-1} of each other. This is consistent with our previous findings that the equilibrium torsional angle of these molecules in both S_0 and S_1 is much closer to 90° than 0°. A relatively small shift in origin frequency is also observed by comparing 9-methylanthracene to 9(2N)A, which suggests that the equilibrium torsional angle of this molecule is significantly different from 0° in S_0 and S_1. The red shift calculated for 9(2N)A (104 cm^{-1}) might even be larger than the true red shift due to the uncertainty in the assignment of the origin (vide supra). In contrast, 2PA and 9VA have origins that are significantly red shifted from those of their methyl derivative counterparts. The origin of 2PA is red shifted by 423 cm^{-1} and that of 9VA by 448 cm^{-1}. Red shifts of this magnitude are consistent with resonance stabilization and, of course, a nearly coplanar geometry ($\phi = 0°$) in one or both of the electronic states involved in the transition.

On the basis of these red shifts, we can immediately make an initial prediction of the correct phase factors for the effective S_1 potentials of 9(2N)A, 2PA, and 9VA. The small red shift of 9(2N)A indicates a nearly orthogonal S_1 geometry. We therefore choose the phase factor so as to place the minor barriers at 90° and 270°, which gives an equilibrium torsional angle of 54° as displayed in Figure 9, rather than a value of 36°, which is obtained by the alternative assignment. In order to obtain planar geometries for 2PA and 9VA, we choose the phase factors so as to place the minima of each of their S_1 potentials at 0° and 180°.

To evaluate the periplanar repulsion, criterion 2, 9(2N)A and 2PA can be compared to other molecules which are structurally similar and for which equilibrium geometries are known. The H atom overlap in 9(2N)A and 2PA is nearly identical with that in 9PA and biphenyl, respectively. In 9PA that overlap is so great as to force an orthogonal ground state geometry and an excited state geometry which is also severely twisted (Figure 8). The similarity of the H atom overlap for 9(2N)A also leads to the prediction of twisted geometries in both states. In fact, our initial prediction for the 9(2N)A S_1 potential has the same qualitative shape as S_1 9PA. Quantitatively, the 0° steric barrier is still the dominant interaction, but the 90° barrier is increased by more than a factor of 2 compared to that in 9PA, indicating an enhanced resonance interaction in 9(2N)A. The H atom overlap in 2PA is much less than in 9(2N)A and should be nearly equivalent to that in biphenyl, which is twisted in S_0 and planar in S_1. Therefore, our initial prediction of a planar S_1 geometry for 2PA is also consistent with steric factors.

In the case of 9VA there is no structurally similar molecule for which the S_1 geometry is known, so our steric evaluation of it is somewhat less certain. Styrene is planar in both S_0 and S_1,[25] but the β-hydrogens are further displayed from the ring H atoms than in 9VA. The overlap of the β-H with nearest neighbor anthracene H atoms is apparently comparable to the H atom overlap in 9PA. However, since the second symmetric interaction of 9PA is missing in 9VA, bond angle deformations that would decrease the H atom overlap might significantly decrease the steric interaction in the planar geometry. The extent to which this mechanism can succeed in stabilizing the planar geometry is uncertain, but it suggests that our initial prediction for the S_1 potential of 9VA is not at variance with steric factors.

Finally, we can show that the phase factors for the S_1 effective potentials of 9(2N)A, 2PA, and 9VA which we have chosen in Figure 9 are consistent with the observation that $S_0 \rightarrow S_1$ excitation constitutes a driving force to planarity in biaryls due to enhancement of resonance interactions in S_1. The phase factors we have chosen for the S_1 potentials of 2PA and 9VA place the minima of each of those potentials at $\phi = 0°$. The alternative assignment gives $\phi = 90°$ for 2PA and 9VA which is inconsistent with the trend toward more planar excited states.

In order for the phase factor chosen for S_1 9(2N)A to be consistent with the trend toward a more planar excited state, we must assume a nearly orthogonal ground state. An S_0 9(2N)A potential with minima at 90° and 270° (like that of 9PA) is consistent with the observed similarity between the torsional progression intensity patterns of 9(2N)A and 9PA and the similar shapes of their respective S_1 potentials.

C. Validity of the Torsional Model. The model based on ascribing a torsional vibration to motion in the single dimension ϕ was quite successful for 9PA[8] and the substituted 9-phenylanthracenes represented in Table VI.[9] The observed torsional frequencies of both S_0 and S_1 9PA were well fitted with just two terms in the Fourier expansion, i.e., eq 3. The phenyl ring deuterium isotope effect was predicted accurately for both S_0 and S_1. In addition, calculated Franck–Condon factors were in good qualitative agreement with observed torsional intensities in the excitation spectrum. Substitution of methyl or fluoro groups at the 3 or 4 phenyl positions of 9PA produced only slight perturbations on the S_1 9PA potential. This is all excellent evidence of pure ϕ motion in these molecules.

This study of 9(2N)A, 2PA, and 9VA lends additional support to the one-dimensional torsional model. The two-parameter function of eq 3 is able to fit the observed vibrational spacings for each molecule, and these effective potentials are consistent with (1) the predicted enhanced resonance interaction in 9(2N)A compared to 9PA, reflected by the larger 90° barrier for S_1 9(2N)A, and (2) less periplanar repulsion in 2PA and 9VA compared to 9PA, reflected by the shift of the 2PA and 9VA S_1 potential minima to 0°.

At the same time, significant failures in the analysis of 2PA and 9VA raise questions about the validity of the one-dimensional torsion model for these molecules. The failures include disagreement between calculated FC factors and observed intensities for 2PA and the discrepancy between the predicted and observed deuterium isotope effects for β-d_2-9VA.

Failure to predict relative transition intensities by FC calculations can be due to a strong dependence of the electronic contribution of the vibronic intensity on which state is being accessed by the transition. Such an effect, which is a breakdown of the Franck–Condon principle, might be expected to be important for torsional vibrations about bonds connecting conjugated groups, since the electronic wave functions for such systems can be strong functions of the torsional angle. A concern which is just as serious, however, is the likelihood that the mode we observe in the spectrum is not pure torsion but vibration which also possessed components of other coordinates such as in-plane and out-of-plane bends, mentioned above. This effect could also explain the small isotope effect observed in β-d_2-9VA. It seems likely that this is due mostly to the symmetry of the nonbonding repulsive interactions. In 9PA, symmetric interactions on both sides of the phenyl ring imply that torsional motion may couple to stretching, but not to bending, of the bond joining the two rings. This symmetry is absent in the cases of the other three molecules, most notably 9VA, in which H–H repulsion is clearly stronger at the β than at the α position. However, even in 2PA and 9(2N)A, where the H–H repulsions on both sides of the ring should be nearly equal, torsional motion which couples to stretching of the bond joining the two rings will also couple to bending of that bond, since the bond does not lie along the line joining the centers of mass of the two rings.

D. Theory for Biaryls. Equilibrium geometries can be calculated quite accurately for saturated molecules by techniques employing empirical force fields and energy minimization.[26]

(24) Friedel, R. A.; Orchin, M.; Reggel, L. *J. Am. Chem. Soc.* **1948**, *70*, 199.

(25) Hollas, J. M.; Khalilipour, E.; Thakur, S. N. *J. Mol. Spectrosc.* **1978**, *73*, 240. Hollas, J. M.; Ridley, T. *Chem. Phys. Lett.* **1980**, *75*, 94.

(26) Williams, J. E.; Stand, P. J.; Schleyer, P. v. R. *Annu. Rev. Phys. Chem.* **1969**, *19*, 531.

However, a realistic treatment of the delocalized π electrons in conjugated molecules requires a more rigorous approach. The equilibrium torsional angle and torsional barrier of biphenyl have been calculated by ab initio molecular orbital theory,[27] but substituted anthracenes represent a significant increase in complexity for those calculations. Semiempirical theories such as CNDO and INDO fail to give qualitatively correct potential functions for rotation about nominally single bonds in conjugated molecules. Improved results are obtained by inclusion of adequate geometry optimization or by retaining more overlap.[28] More accurate theories have been used recently which are hybrids of the empirical and semiempirical methods.[29]

Of the substituted anthracenes we have studied, S_0 9PA is the only one for which an equilibrium torsional angle has been calculated experimentally.[30] The value obtained was 67° instead of the experimentally derived value of 90°. Equilibrium torsional angles and torsional barriers have been calculated for other biaryls,[18,19,20,27,31] but usually good experimental information for comparison is lacking. We believe that our LIF experiments on substituted anthracenes, along with a limited number of other LIF examples (e.g., tolane[10c]), now yield sufficiently accurate torsional potentials for biaryls to provide a fresh stimulus and points of reference for future work in this field.

Acknowledgment. The authors are indebted to Professor Clayton F. Giese for providing the pulsed beam source and to Dr. Jaan Laane for giving us a copy of the computer code[32] which was used to determine the best-fit torsional potential parameters. A.M.B. was 1983-1984 Amoco Predoctoral Fellow. The research was supported by the National Science Foundation Grant No. CHE-8319930, CHE-8205769, and CHE-8351158 and by the Graduate School of the University of Minnesota.

Registry No. 9VA, 2444-68-0; 9(2N)A, 7424-72-8; 2PA, 1981-38-0; 9-methylanthracene, 779-02-2; 2-methylanthracene, 613-12-7.

Supplementary Material Available: Tables of assignments of the 9(2N)A, 2PA, and 9Va fluorescence excitation spectra (8 pages). Ordering information is given on any current masthead page.

(27) Almlöf, J. *Chem. Phys.* **1974**, *6*, 135.
(28) Birner, P.; Hofmann, H.-J. *Int. J. Quantum Chem.* **1982**, *21*, 833.
(29) Warshel, A.; Karplus, M. *J. Am. Chem. Soc.* **1972**, *94*, 5612. Carter, R. E.; Liljefors, T. *Tetrahedron* **1976**, *32*, 2915.
(30) Hofmann, H.-J. *Z. Chem.* **1975**, *15*, 76.
(31) Gustav, K.; Kemka, U.; Sühnel *J. Mol. Struct.* **1981**, *86*, 181.
(32) Lewis, J. D.; Malloy, T. B., Jr.; Chao, T. H.; Laane, J. *J. Mol. Struct.* **1972**, *12*, 427.

^{31}P NMR Study of Trialkylphosphine Probes Adsorbed on Silica-Alumina

Laima Baltusis, James S. Frye, and Gary E. Maciel*

Contribution from the Department of Chemistry, Colorado State University, Fort Collins, Colorado 80523. *Received December 26, 1985*

Abstract: Three trialkylphosphines have been investigated as probe molecules for the study of acidic sites on amorphous silica-alumina. These molecules incorporate many favorable NMR features, such as high sensitivity of the ^{31}P nuclide, high natural abundance, and short relaxation times, which allow convenient quantitative studies of acidic sites on surfaces. Phosphines bound at Brønsted and Lewis sites have been distinguished by chemical shift analogies to model systems. Unlike some other spectroscopic methods that typically measure both surface and bulk sites, the analysis of amorphous materials by probe molecules such as phosphines results in the detection of acidic sites that are strictly on the surface and thus catalytically accessible. Variation of the surface phosphine concentration yields a titration of acidic sites. At low phosphine concentrations only phosphines bound to Brønsted sites are observed. As the phospine concentration is increased, phosphines bound to Lewis sites and physisorbed phosphines appear simultaneously. Because of the relatively large chemical shift separation of Brønsted bound phosphines from all other phospine chemical species, it is possible to assay the absolute numbers of surface Brønsted sites directly. Different phosphines count different numbers of Brønsted sites, demonstrating the desirability of using more than one type of probe molecule to characterize surfaces with specific binding sites. It has not been possible to quantitate the number of Lewis sites on silica-alumina because of small differences in chemical shifts and binding constants of Lewis-complexed and physisorbed phosphines. Variable-temperature studies have shown phosphine surface species to be in slow chemical exchange with one another, in contrast to the case of pyridine as a probe molecule previously studied by ^{15}N and ^{13}C NMR.

The catalytic activities of aluminosilicates (e.g., zeolites and amorphous silica-alumina) have inspired a wealth of studies designed to characterize the active sites. The charge-compensating protons (Brønsted sites) adjacent to the tetrahedral aluminate anionic centers in the lattice and tricoordinate neutral aluminum centers (Lewis sites) are believed to be important catalytic sites of aluminosilicates.[1-4] Numerous chemical methods have been developed to determine the numbers and types of surface active sites; these methods include aqueous titrations, nonaqueous titrations, calorimetric measurements, and model cracking reactions. Spectroscopic methods that have been applied in the study of these materials include X-ray fluorescence, infrared, and nuclear magnetic resonance.[1-4] With new developments in high-resolution multinuclear solid-state NMR, the number of NMR investigations of amorphous materials has steadily increased, with a particular emphasis on the study of surface-related phenomena of such materials.[5,6]

Various NMR approaches have been used in attempts to characterize acidic sites in aluminosilicates. There have been many

(1) Goldstein, M. S. In *Experimental Methods in Catalytic Research*; Anderson, R. B., Ed.; Academic Press: New York, 1968; p 361.
(2) Tanabe, K. *Solid Acids and Bases*; Academic Press: New York, 1970.
(3) Forni, F. *Catal. Rev.* **1973**, *8*, 69.
(4) Benesi, H. A.; Winquist, B. H. C. *Adv. Catal.* **1978**, *27*, 98.
(5) Duncan, T. M.; Dybowski, C. *Surf. Sci. Rep.* **1981**, *1*, 157.
(6) Howe, R. F. In *Chemistry and Physics of Solid Surfaces V*; (Vanselow, R., Howe, R., Eds.; Springer-Verlag: Berlin, 1984; p 39 and references therein.

0002-7863/87/1509-0040$01.50/0